

Toward a dynamic topographic components model

André Achim*, Sylvie Bouchard

Laboratoire de Neurosciences de la Cognition, Université du Québec à Montréal, Montréal, Canada

Accepted for publication: 9 January 1997

Abstract

Möcks' topographic component model (TCM) (Möcks, J. Topographic components model for event-related potentials and some biophysical considerations. *IEEE Trans. Biomed. Eng.*, 1988a, 35: 482–484; Möcks, J. Decomposing event-related potentials: a new topographic components model. *Biol. Psychol.*, 1988b, 26: 199–215) decomposes event-related potentials into components uniquely determined by their respective amplitude profiles across replicates, assuming a constant topography and wave shape for each component. To accommodate possible changes in the component expression across conditions, a dynamic version of TCM is investigated which further admits component modulation in time scale. Twenty test problems were synthesized, incorporating two arbitrary topographies each activated with its own arbitrary wave shape modified, across two conditions, in amplitude, onset and duration. Seventeen problems were perfectly solved, with substantial success on the remaining three, confirming that component jitter or stretching can even help component identification. © 1997 Elsevier Science Ireland Ltd.

Keywords: Topographic component model; Event-related potentials; Component jitter

1. Introduction

Event-related potentials (ERPs) are often conceptualized as sums of components each showing (a) a characteristic behavior over time, (b) a topographic distribution reflecting the cerebral structures emitting them and, eventually, (c) selective reactivity to experimental conditions. Few mathematical decomposition techniques have systematically exploited the latter characteristic. Principal component analysis (PCA) of ERPs (Donchin and Heffley, 1978) uses the experimental variability without distinguishing it from spatial variability. Similarly, multiple dipole modeling interpretations of ERPs, like results from the BESA software (Scherg, 1990), may require the same dipoles to explain the data from multiple conditions, but does not generally use a constraint that the same component should have a similar behavior across conditions. Turetsky et al. (1990) described a model in which all components were forced to have the same generic time course, a damped sinusoid, with different expression parameters across components or conditions, again with no constraint concerning any specific

similarity of response of each given component across conditions.

A notable exception, in terms of capitalizing on a constraint that each component should retain its activity pattern across replicated spatio-temporal ERPs (ST-ERPs), is Möcks' topographic component model (TCM) (Möcks, 1988a,b). TCM is analogous to PCA, although with one extra dimension. While PCA reproduces the cases (all the existing combinations of channels, subjects and conditions) by appropriately weighted sums of an efficient set of temporal components (i.e. basis wave shapes), TCM mathematically expresses its cases (all existing combinations of subjects and conditions) by appropriately weighted sums of a few basic spatio-temporal components, each resulting from crossing one appropriate topography with one appropriate wave shape. Just as component wave shapes in PCA are model-free, in TCM both the topographies and the wave shapes are model-free, being algorithmically derived to account for as much data variance as possible for a given number of components.

Contrary to PCA decomposition, TCM forces each basic wave shape to have the same spatial profile across the various ST-ERPs. Conversely, just as PCA can be applied in the spatial domain instead of the temporal domain, one could say that TCM forces each basic topography to have

* Corresponding author. LNC/UQAM, C.P. 8888, Succursale Centre-Ville, Montréal, Québec, H3C3P8, Canada. Tel.: +1 514 9873000, ext. 8435; fax: +1 514 9878952; e-mail: achim.andre@uqam.ca

the same wave shape, except for its amplitude, across all cases. The restriction, imposed by TCM, that each component must have both a constant spatial profile and a constant temporal profile gives it the valuable property that the least squares solution is unique for a fixed number of components. It is typical that PCA is followed by a Varimax rotation in search of more easily interpretable components that would explain the same total variance, although with a different partitioning across components. A TCM solution, however, should be directly interpretable if the number of components is correct. It is not subject to subsequent rotation. Indeed, forming linear combinations of TCM components would produce invalid TCM components, i.e. spatio-temporal matrices that cannot be reproduced by crossing a single topography with a single wave shape.

TCM could thus become a preliminary step in multiple source localization on related ST-ERP data, whenever a source may be expected to correspond in time with an ERP component and in space with the topography of its generator. Since TCM should be able to identify uniquely the actual source topographies without recourse to any physical modeling, it could eventually help circumvent the severe problems associated with model misspecification (Zhang and Jewett, 1993; Zhang et al., 1994).

While, in principle, TCM should directly uncover the topography, the wave shape and the amplitude profile across cases of each component, it must be emphasized that this is strictly dependent on the condition that the assumptions of the model are satisfied. Firstly, the components must have a constant topography across conditions, which is reasonable in many practical situations. Secondly, they must also have a constant wave shape. While this is also often reasonable, it excludes all cases where the experimental conditions affect the onset latency or the duration of some components. For instance, in selective auditory attention studies, the processing negativity is longest for non target stimuli most similar to the target. Finally, to be uniquely identifiable, the components must have different amplitude profiles across cases. An experimental manipulation that would simply decrease or increase the amplitude of all the components in the same proportion would merely provide scaled copies of the same ST-ERP, lacking the information required to correctly recover the cerebral components from which the ERPs emanate.

Field and Graupe (1991) were the first and apparently only researchers to publish an application of TCM to actual ST-ERPs. TCM being formally equivalent to the PARAllel FACtors (PARAFAC) model (Harshman, 1970), they used the PARAFAC analysis package (Harshman and Lundy, 1984a,b) to explore practical issues in TCM analysis. ST-ERP signals from checkerboard reversals were replicated over subjects, as in Möcks' original formulation. This might have poorly satisfied the third requirement above, with little variability across subjects in the relative amplitude among the true underlying components. Their solution involved three components, was obviously laborious to

reach, and required the compromise of imposing orthogonality among the wave shapes. The three topographies were all very highly inter-correlated (all three sums of cross products of normalized topographies were above 0.98, analogous to having a correlation above 0.98 between any pair) and at least one of the three wave shapes (component 2) showed a complex pattern (with consecutive peaks not separated by a zero crossing) which casts doubts on its validity. Component 3 was interpreted as accounting for temporal jitter in component 2, but it had a simpler temporal pattern, which makes this interpretation hard to maintain. This practical application of TCM has not proved inspiring to other researchers.

The theoretical advantages of TCM, however, call for further investigation. Improvement relative to the third requirement could be obtained by replacing the subjects by a set of experimental conditions known to modify the relative intensity of some components more than that of other components. But improvement of the mathematical model itself may also be contemplated. In particular, TCM could possibly be adapted relative to the second requirement, to allow for time scale variations in the expression of the individual components across conditions. Toward this end, we investigated the possibility of solving ST-ERP problems that would obey the following formal description: (a) ST-ERPs were obtained under at least two conditions; (b) the ST-ERPs were produced by the same set of dynamic spatio-temporal components (DSTC); (c) each DSTC is characterized by one constant topography, one constant prototype wave shape, and three expression parameters (amplitude, onset and duration); and (d) the analysis epoch includes the whole activation of each component (i.e. both ends of the ERPs are at base line in all channels).

The purpose of the present work was to demonstrate that such problems are indeed manageable and, therefore, it is worth channeling R and D efforts toward more efficient and more general approaches. In particular, the method used here requires that the components differ in topographies, which is not a necessary requirement of TCM. Furthermore, the present method would not easily generalize to more than two conditions. These restrictions, however, should be of little concern at this early stage of development of analysis models that can recognize components even if they are modified in onset or duration across conditions. While such temporal variations are nuisances in PCA, requiring the inclusion of extra components, dynamic TCM models not only accommodate them, but they actually use them toward correctly identifying the contributing components.

2. Methods

2.1. Data generation

Twenty data sets were synthesized, each representing two ST-ERPs embodying different expressions of the same two

components. Different topographies and associated wave shapes were generated for each data set, and different expression parameters were generated for the wave shape of each component in each condition. Letting $T(i,c)$ be the value of the topography of component i at channel c , $P(i,r)$ be the prototype wave shape of component i , with null values outside the range $0 \leq r \leq 1$, and a_{ij} , o_{ij} and d_{ij} be the expressed amplitude, onset, and duration of component i in condition j , then the observed spatio-temporal data for condition j , channel c , time t are

$$D(j, c, t) = \sum_i T(i, c) a_{ij} P((t - o_{ij}) / d_{ij})$$

For ease of representation, the topographies corresponded to a single line of electrodes, which is not restrictive since electrode positions are not used by the method. They were generated for 16 equidistant channels by assigning normally distributed random weights to the first four powers of x from -1 to $+1$, summing and normalizing the amplitudes to unit sum of squares. A pair of such topographies constitutes the first row of Fig. 1. The associated prototype wave shapes were similarly produced over 100 time points, but were further weighted by $1 - x^2$ (a parabolic window reducing the amplitude to zero at both ends). For each component in each condition, the prototype wave shape was shrunk, by cubic spline interpolation, between random onset and offset values in the ranges $0.0-0.3$ and $0.5-1.0$, respectively, and assigned a random amplitude uniformly distributed in the range $2.0-3.0$. The second and third rows of Fig. 1 show the expression of two prototypes (rows) in the two conditions (columns). The last 16 rows show the resulting data at successive channels in each condition. Consecutive integers from 201 to 220 were used as seeds for generating the 20 test problems. Data sets with topographies correlating above 0.95 were replaced by adding 100 to the original seed.

2.2. Analysis

SVD on the two ST-ERPs end to end could confirm that two topographies were sufficient to reproduce the data perfectly; this follows from the fact that the data at each latency in each condition were generated as weighted sums of only two topographies. The topographies thus identified by SVD served as initial approximations for the decomposition algorithm. The general strategy is (a) to use a hypothesis about the topographies to obtain what their activation should be in each condition, (b) to replace, separately for each component, the individual wave shapes across conditions by a common prototype wave shape appropriately adjusted in onset, duration and amplitude (this critical step is described below), (c) to use these reproduced wave shapes across conditions to obtain a better estimation of the component topographies, and (d) to repeat the estimation cycle until all the values of each topography and each wave shape change less than an arbitrarily small amount between consecutive evaluations.

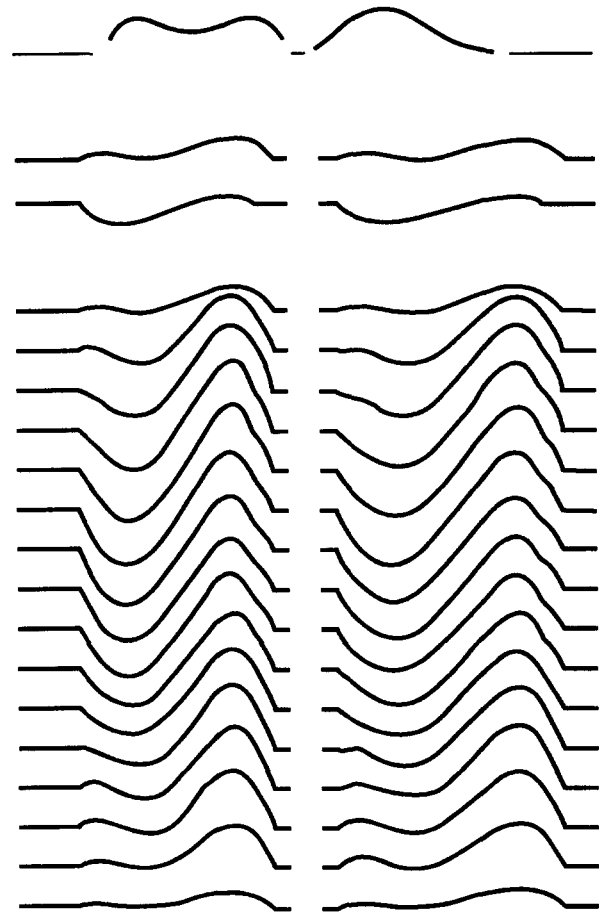


Fig. 1. Generating components and resulting data for test problem #12. The first row illustrates the two source topographies (16 aligned channel positions, for ease of illustration) embedded between base lines indicating the zero level. For all following rows, the two columns correspond to two different experimental conditions. Rows 2 and 3 present the activation wave shapes respectively associated with the left and right topographies of the first row. The last 16 rows represent the resulting signal at each of the 16 consecutive channels, and constitute the data subjected to analysis.

Technically, at each iteration, the pseudo-inverse of the matrix of topographies was applied to the data (with the two conditions put end to end) to obtain the corresponding best-fit wave shapes (BFWS) in each condition. The next step involved resampling, by spline interpolation, the two wave shapes of a given component, using non linear optimization to identify the parameters that best equalize their time scales under parametric control. For this, only two time modulation parameters were required, i.e. their relative start time (RST) and relative end time (RET). They were adjusted such that the two time-corrected BFWS were maximally reproduced by projecting each on their average. Although two start times and two end times are required to renormalize the timing of a component in two conditions, the approach adopted here requires only two parameters. If the RST parameter is positive, its value is used as a new start time for condition 1 and the data start time is used for condition 2. If, however, the relative onset is negative, then the data start time is used for condition 1 and $-RST$ is used

as a new start time for condition 2. A similar approach is used with RET, except that the other end of each wave shape is considered.

Having obtained the best RST and RET for a given component, the average of the corresponding time corrected BFWS was normalized in amplitude and became the prototype estimate for that component. The amplitude with which it was expressed with the appropriate time correction in each condition was determined by linear algebra. The BFWS of each component were then replaced by the current prototype modified according to its estimated expression parameters, with the two conditions again put end to end to form a single wave shape for each component. The pseudo-inverse of these wave shapes was then applied to the two data ST-ERPs attached end to end to obtain a new and improved estimate of the corresponding topographies. The iteration process was subject to a maximum of 500 cycles, in case the convergence criterion would fail to be reached (e.g. eventual alternation between the same two solutions). An occasional perturbation was imposed on the converging process, under the control of monitoring criteria, to prevent the solution degeneracy described by Field and Graupe (1991). This perturbation of the converging sequence consisted of replacing the current two topographies by their sum and their difference respectively, when the current normalized topography estimates projected on one another with a weight above 0.95 in absolute value and their normalized reproduced wave shapes projected above 0.95 in the opposite direction. The residuals were also monitored. When they failed to improve between consecutive iterations, alternate values were tried for a step size parameter controlling the optimization of RST and RET; this was often successful.

3. Results

The correlation (projection) between the two component topographies ranged from 0.0033 to 0.9476 in absolute value, with a median of 0.6483. When the expressed component wave shapes over the two conditions were put end to end and normalized, their mutual projection ranged, over the 20 test problems, from 0.0018 to 0.8762 in absolute value, with a median of 0.5211.

Seventeen of the 20 problems were solved essentially perfectly, i.e. the reproduced topography and prototype of each source was superimposed to the original ones on the computer screen and more than 99.995% of the data sum of squares was reproduced. In two other data sets, the topography of one component and the wave shape of the other were reproduced perfectly, which suggests that the monitoring criteria failed to recognize the need to impose the perturbation described above. One of them had a spatial correlation between components of 0.9476 and between temporal components (conditions end to end) of 0.5804; the other had respective correlations of 0.5233 and 0.5232. The remaining

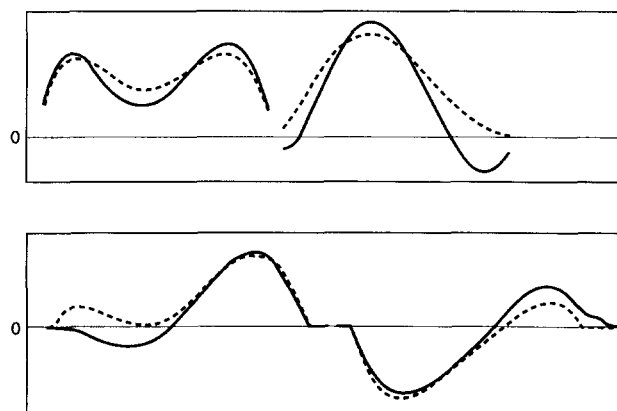


Fig. 2. Ideal (dashed lines) and reproduced (solid lines) topographies (top) and prototype wave shapes (bottom) for the data depicted in Fig. 1. This problem represents the worst case among the 20 test problems, in that both topographies and both prototype wave shapes are only approximately reproduced. They were essentially perfectly reproduced in 17 problems; in two other problems, only the topography of one source and the prototype wave shape of the other source were perfectly reproduced. For this problem, the solution topographies projected 0.921 and 0.977, respectively, on their target topographies (equivalent to correlation coefficients, but without removing the means), and the solution prototype wave shapes projected 0.951 and 0.901, respectively, on their target wave shapes.

problem is the one illustrated in Fig. 1. It had spatial and temporal correlations between its two components of 0.8098 and -0.0018 , respectively. The topographies and prototype wave shapes were reasonably approximated but were not superimposed on the original ones despite 99.98% of the data sum of squares being reproduced (Fig. 2). The cause for this is not yet diagnosed. We note that high spatial correlation or low temporal correlations between the two components are not specific predictors of imperfect solutions. Problem 17, for instance, had respective correlations of 0.9313 and 0.0026 and was perfectly solved.

4. Discussion

Although the data were somehow idealized, with only two sources and no noise, the problems solved by the decomposition method were extremely difficult from the point of view of PCA, even if followed by oblique rotation rather than Varimax. The high success of the procedure seems to confirm that substantial decomposition power may be derived from a formal model of ST-ERP which uses component variation not only in amplitude but also in onset and duration times.

Before applying the method to practical problems, further work should extend the method to more than two replicates and more than two components, including some components that are not affected at all by experimental condition. Also, the robustness of the method to noise correlated in time and space must be established. This will likely call for further improvements of the algorithm. The present exploration, however, suggests that further work in this direction

will likely lead to a generation of useful new tools for deciphering the brain processes reflected in ST-ERPs.

Acknowledgements

This research was supported by a fellowship from the Fonds de Recherche en Santé du Québec and by a grant from the National Science and Engineering Research Council of Canada to the first author.

References

- Donchin, E. and Heffley, E.F. Multivariate analysis of event-related potential data: a tutorial review. In: D.A. Otto (Ed.), *Multidisciplinary Perspectives in Event-Related Brain Potential Research*. US Environmental Protection Agency, Washington, DC, 1978, pp. 555–572.
- Field, A.S. and Graupe, D. Topographic component (parallel factor) analysis of multichannel evoked potentials: practical issues in trilinear spatiotemporal decomposition. *Brain Topogr.*, 1991, 3: 407–423.
- Harshman, R.A. Foundation of the PARAFAC procedure: models and conditions for an 'explanatory' multi-mode factor analysis. *UCLA Working Paper in Phonetics*, 1970, 16: 1–84.
- Harshman, R.A. and Lundy, M.E. The PARAFAC model for three-way factor analysis and multidimensional scaling. In: H.G. Law et al. (Eds.), *Research Methods for Multimode Data Analysis*. Praeger, New York, 1984a, pp. 122–215.
- Harshman, R.A. and Lundy, M.E. Data preprocessing and the extended PARAFAC model. In: H.G. Law et al. (Eds.), *Research Methods for Multimode Data Analysis*. Praeger, New York, 1984b, pp. 216–284.
- Möcks, J. Topographic components model for event-related potentials and some biophysical considerations. *IEEE Trans. Biomed. Eng.*, 1988a, 35: 482–484.
- Möcks, J. Decomposing event-related potentials: a new topographic components model. *Biol. Psychol.*, 1988b, 26: 199–215.
- Scherg, M. Fundamentals of dipole source potential analysis. In: F. Grandori, M. Hoke and G.L. Romani (Eds.), *Auditory Evoked Magnetic Fields and Electric Potentials*. *Advances in Audiology*, Vol. 6. Karger, Basel, 1990, pp. 40–69.
- Turetsky, B., Raz, J. and Fein, G. Representation of multi-channel evoked potential data using a dipole component model of intracranial generators: application to the auditory P300. *Electroenceph. clin. Neurophysiol.*, 1990, 76: 540–556.
- Zhang, Z. and Jewett, D.L. Insidious errors in dipole localization parameters at a single time point due to model misspecification of number of shells. *Electroenceph. clin. Neurophysiol.*, 1993, 88: 1–11.
- Zhang, Z., Jewett, D.L. and Goodwill, G. Insidious errors in dipole parameters due to shell model misspecification using multiple time points. *Brain Topogr.*, 1994, 6: 283–298.